HHS Public Access

Author manuscript

Phys Med Biol. Author manuscript; available in PMC 2017 November 07.

Published in final edited form as:

Phys Med Biol. 2016 November 7; 61(21): 7639–7651. doi:10.1088/0031-9155/61/21/7639.

A Multiplexed TOF and DOI Capable PET Detector Using a Binary Position Sensitive Network

M F Bieniosek[1,2,4], **J W Cates**[1,2], and **C S Levin**[1,2,3,4,5]

C S Levin: cslevin@stanford.edu

[1]Department of Radiology, Stanford University, Stanford, CA 94305, USA

[2]Molecular Imaging Program at Stanford (MIPS), Stanford, CA 94305, USA

[3]Department of Physics, Stanford University, Stanford, CA 94305, USA

[4]Department of Electrical Engineering, Stanford University, Stanford, CA 94305, USA

[5]Department of Bioengineering, Stanford University, Stanford, CA 94305, USA

Abstract

Time of flight (TOF) and depth of interaction (DOI) capabilities can significantly enhance the quality and uniformity of positron emission tomography (PET) images. Many proposed TOF/DOI PET detectors require complex readout systems using additional photosensors, active cooling, or waveform sampling. This work describes a high performance, low complexity, room temperature TOF/DOI PET module. The module uses multiplexed timing channels to significantly reduce the electronic readout complexity of the PET detector while maintaining excellent timing, energy, and position resolution. DOI was determined using a two layer light sharing scintillation crystal array with a novel binary position sensitive network. A 20mm effective thickness LYSO crystal array with four 3mm × 3mm silicon photomultipliers (SiPM) read out by a single timing channel, one energy channel and two position channels achieved a full width half maximum (FWHM) coincidence time resolution of 180 ± 2ps with 10mm of DOI resolution and 11% energy resolution. With sixteen 3mm × 3mm SiPMs read out by a single timing channel, one energy channel and four position channels a coincidence time resolution 204 ± 1ps was achieved with 10mm of DOI resolution and 15% energy resolution. The methods presented here could significantly simplify the construction of high performance TOF/DOI PET detectors.

1. Introduction

Time of flight (TOF) positron emission tomography (PET) uses very precise measurements of 511 keV photon interaction times to position annihilation events within system detector lines of response (Mullani, Markham & Ter-Pogossian 1980) (Gariod, Allemand, Cormoreche, Laval & Moszynski 1982) (Karp, Surti, Daube-Witherspoon & Muehllehner 2008) (Levin 2008) (Moses 2007). TOF can greatly improve PET image quality. For example a PET image using 2D reconstruction has a signal to noise ratio (SNR) improvement from TOF given by the formula (Budinger 1983):

$$SNR_{\text{increase}} = \sqrt{\frac{2D}{c\Delta t}} \quad (1)$$

Where D is the diameter of the patient, Δt is the coincidence timing resolution of the scanner, and c is the speed of light. Thus, improvements in PET time resolution can directly lead to increased PET image quality.

Depth of interaction (DOI) PET detectors have the ability to determine the depth within a PET detector of 511 keV photon interactions. For high sensitivity, most PET scanners require thick detectors to give the required 511 keV stopping power. However, uncertainty in the depth of interactions within thick detectors can lead to parallax errors (Levin 2008). This parallax degradation increases with radial position within the PET field of view. For high performance TOF detectors, where the TOF kernel size approaches the scintillation crystal size, DOI can also help accurately place TOF kernels during image reconstruction by reducing the uncertainty in the LOR endpoints (Spanoudaki & Levin 2011).

Several methods have been proposed to construct TOF/DOI PET detectors which require an increase in PET detector complexity. Many designs have an increased number of photosensors such as dual-ended readout (Kang, Ko, Rhee, Kim, Lee & Hong 2015), or multi-layered detectors (Yeom, Vinke & Levin 2014). Other methods do not use increased number of photodetectors such as using scintillation shape (rise or decay times) (Schmall, Surti & Karp 2015) (Roncali, Schmall, Viswanath, Berg & Cherry 2014) or light sharing (Van Dam, Borghi, Seifert & Schaart 2013) (Ito, Lee & Lee 2013) to give DOI information. However, many of these methods require active cooling or a significant increase in PET detector readout complexity to measure the light spread or scintillation shape accurately.

This work describes a TOF/DOI PET detector that uses multiplexing and a binary position sensitive network to significantly simplify the PET detector readout. Multiplexing allows the acquisition of PET data from many photodetectors using fewer readout channels. Previously published multiplexing methods include light sharing (Kim, McDaniel, Malaney, McBroom, Peterson, Tran, Guo, Ivan, Dolinsky, Wagadarikar et al. 2012) or charge sharing (Vinke, Yeom & Levin 2015) (Kwon & Lee 2014) (Downie, Yang & Peng 2013) (H.-J. 2014) (Kim, Chen, Eclov, Ronzhin, Murat, Ramberg, Los, Wyrwicz, Li & Kao 2015). Multiplexed detectors using SiPM photodetectors can also maintain excellent timing properties while significantly reducing the number of readout channels (Bieniosek, Cates & Levin 2016) (Bieniosek, Cates, Grant & Levin 2016). To reduce timing degradation due to increased dark counts, proper filtering or baseline correction of the SiPM signal must be performed. In this work a multiplexed readout of a two layer light sharing scintillation crystal array was used to create a significantly simplified TOF/DOI PET detector.

2. Methods

2.1. Multiplexed Timing Channel

As described in (Bieniosek, Cates & Levin 2016) and (Bieniosek, Cates, Grant & Levin 2016) SiPM timing signals can be multiplexed with minimal timing degradation. In this work the multiplexed SiPM cathodes were directly connected. These cathodes were then coupled to the timing readout channel using a 10pF capacitor (see Figure 1). The 10pF capacitor coupled to a 50 Ohm readout channel accepts high frequency signals required for timing measurements, while low frequency signals are read out by the energy channel. The fast rising leading edge from this readout channel provides an excellent timing signal.

2.2. Multiplexed Energy Channel

In order to maintain energy resolution, a low frequency energy channel was placed in parallel with the high frequency timing channel coupled to the readout electronics with a 100nF capacitor in series with a 500 Ohm resistor (see Figure 1). The 500 Ohm resistor blocks signals at high frequencies when the impedance of the 10pF timing channel capacitor is very low. At low frequencies when the impedance of the 10pF capacitor is high, the energy channel receives the current from the SiPMs.

2.3. DOI Crystal Array and Binary Position Sensitive Network

In this work, a light sharing two layer lutetium-yttrium oxyorthosilicate (LYSO) scintillation crystal array is used to give DOI information (see Figure 2). The bottom layer of the crystal array is a 4×4 array of 3mm × 3mm × 10mm rectangular prisms. This layer was designed to couple one to one with a 4×4 monolithic Hamamatsu S13361-3050AE SiPM array. The top layer of the crystal array consists of triangular prisms that are optically coupled to the lower layer of crystals. Due to the geometric differences between the two layers each crystal in the two layers will have a unique distribution of light projected onto the SiPM array. Light from bottom layer scintillation events will primarily be sensed by the SiPM directly beneath the crystal. Light from top layer scintillation events will primarily be shared between the two SiPMs beneath it.

In order to sense the distribution of charge on the SiPM array a position sensitive network was used. Many position sensitive networks use resistive mesh networks that have a pincushion distortion due to unequal impedances to readout channels between different SiPMs. The light sharing crystal arrays used in this work have a particularly severe pincushion distortion, because light from any crystal can be shared with a corner pixel that is more heavily weighted in a resistive mesh position sensitive network. A binary position sensitive network with identical impedances seen by each SiPM was used to avoid pincushion distortion while maintaining excellent timing and position resolution (see Figure 1).

In the binary position sensitive network presented in this work each multiplexed SiPM cathode is connected to a common energy and timing channel. Each anode is connected to ground through a small 20 Ω resistor. A small resistance is needed to minimize high frequency shaping of the timing signal. Each anode is also connected to split off 100 Ω

resistors that are either connected or not connected to position channels in unique combinations. Split off resistors not connected to a position channel are connected to dummy resistors with the same impedance as the position channels. Thus each SiPM will see the same impedance to ground, and the same impedance to any connected position channels, eliminating pincushion distortion in the flood map. For a binary network multiplexing 4 SiPMs, two split off channels are required to uniquely identify each SiPM (referred to as a ’2 bit’ binary network), for 16 SiPMs, four split off channels are required (referred to as a ’4 bit’ binary network). This unique combination for each SiPM will be referred to as the SiPM’s binary code. For example an SiPM in a two bit network connected to both position channels has the code ’11’, while the SiPM connected to both dummy resistors has the code ’00’.

In order to show that the scintillation crystal where an PET event occurs can be identified, flood maps were produced. Flood maps show the distribution of sensed PET event locations. PET events from a single crystal should be clustered near each other. The separation between clusters shows with what probability an event’s crystal can be identified. Flood maps from the binary position sensitive network were produced by simply plotting the integrated magnitude of the first 60ns of each position channel waveform. A 2 bit binary network will have a 2 dimensional flood map (one dimension for each position channel). The flood map of a 4 bit binary position sensitive network has 4 dimensions (one for each position channel). In this work, a series of of 2D flood maps were produced in order to display 4D flood maps.

It is important to note that when choosing the codes for each SiPM for a binary position sensitive network, care must be taken to optimize the separation between crystals in the flood map. Bottom layer crystal positions in the flood map can be described with the binary code of the SiPM they are coupled to. Top layer crystals share light between two SiPMs, so their flood map position can be described by the average of the two SiPM codes. Some configurations can lead to overlapping top layer crystal positions, or codes that lead to non-optimal flood map distances between crystals (see Figure 3). For a two bit binary network each crystal can be separated by at least $\frac{1}{2}$ the distance between neighboring bottom layer crystals, for a four bit network crystals can be separated by at least $\frac{1}{\sqrt{2}}$ the distance between neighboring bottom layer crystals. The codes used in this work are seen in Figure 4.

2.4. Experimental Setup

To test our multiplexed TOF/DOI PET module, the light sharing LYSO crystal array described in the Position and DOI Information Section was coupled to a Hamamatsu S13361-3050AE monolithic 4×4 array of 3mm × 3mm SiPMs. The S13361-3050AE SiPMs have low dark count and afterpulse rates which were theorized to be beneficial for multiplexed timing resolution as described in (Bieniosek, Cates & Levin 2016) and (Bieniosek, Cates & Levin 2015).

DOI was studied by creating flood maps with the crystal array oriented head on with a reference crystal, with only the top-layer crystals in coincidence with a reference crystal, and

with only the bottom-layer crystals in coincidence with a reference crystal. Coincidence timing experiments were then performed with 2 bit and 4 bit binary networks as seen in Figure 5. In the 2 bit experiments only one quadrant of the SiPM and crystal arrays were characterized. In the 4 bit experiments the full 4×4 array of SiPMs and 32 crystals were characterized. In all of the coincidence timing experiments two identical detector modules were measured in coincidence.

Timing channels were amplified with a mini-circuits ZX60-4016E-S+ preamplifier (one per module) and read out by an Agilent 2.5GHz 20Gsa/s Oscilloscope. Timing pickoff was performed with a cubic spline interpolation and a leading edge threshold of the digitized timing waveform. Energy channels (one per module) were digitized without amplification by the Agilent Oscilloscope and the maximum voltage was used to determine the interaction energy. Position channels (2 per module for 2 bit network, 4 per module for 4 bit network) were digitized without pre-amplification by a Caen V1742 Digitizer. The integral of the first 60 ns of the position signals after the timing trigger was used as the position channel magnitude. Finally, a coincidence timing experiment was also performed with an Analog Devices ADCMP572 comparator time pickoff, to show that high speed waveform digitization is not required for good timing performance. In the comparator timing pickoff experiments the Agilent Oscilloscope was used as the time to digital converter of the comparator signal (see Figure 6). All experiments were performed at room temperature with no thermal regulation.

3. Results

Flood maps for the 2 bit binary configuration were taken with the two layer DOI LYSO crystal array collimated with head on irradiation, collimated to the the center of the top layer crystals, and collimated to the center of the bottom layer crystals (see Figure 7). Flood maps were produced by plotting a 2 dimensional histogram of the distribution of position channel 1 and position channel 2 magnitudes (no anger logic is necessary). All 8 crystals are seen, well separated in the flood map. In the bottom layer collimated flood map, bottom layer crystals appear in their expected positions (for example, the crystal over the ’11’ SiPM appears in the top right because both position channels 1 and 2 have a high magnitude, while the crystal over the ’00’ SiPM appears in the bottom left because both position channels 1 and 2 have low magnitudes). In the top layer collimated flood map, the top layer crystals appear between the bottom layer crystals with which they share light. Thus the detector array has position and DOI information.

The 2 bit binary coincidence time resolution measurement with 4 SiPMs multiplexed to a single timing channel and readout by the high performance waveform digitizer showed a coincidence time resolution of 180 ± 2ps full width half maximum (FWHM) (see Figure 8). Coincidence photon interactions that occurred in the bottom layer of both detectors had a time resolution of 185 ± 3ps, while coincidence pairs that occurred in the top layer of both detectors had a time resolution of 170 ± 2ps. With time pickoff performed with an Analog Devices ADCMP572 comparator chip the coincidence time resolution was 190 ± 3ps FWHM, only slightly worse than that measured with the high performance waveform digitizer (see Figure 9). Energy resolution was 11%, and the flood map showed all 8 crystal

separated with crystal centroid distance to centroid standard deviation ratio of 9.2 (see Figure 10). All error bars are one standard deviation Gaussian fitting errors.

The 4 bit binary coincidence time resolution measurement with 16 SiPMs multiplexed to a single timing channel showed a time resolution of 204 ± 1ps FWHM using the waveform digitizer (see Figure 11). Coincidence pairs that occurred in the bottom layer of both detectors had a time resolution of 221 ± 3ps, while coincidence pairs that occurred in the top layer of both detectors had a time resolution of 194 ± 4ps. Energy resolution was 15%, and the flood map showed all 32 crystal separated with crystal centroid distance to centroid standard deviation ratio of 7.2 (see Figure 12).

4. Discussion

The multiplexed TOF/DOI modules presented in this work show excellent timing performance in both DOT layers (see Figures 8 and 11). The excellent timing resolution was achieved with either a high performance sampling oscilloscope that captures the waveform of each pulse, or with an off-the-shelf chip-based comparator performing the time pickoff (see Figure 9). This simple architecture shows that the proposed TOF/DOI timing scheme can be easily scaled to larger systems. An entirely passive binary positioning network provided positioning information, including DOI (see Figures 7, 10, and 12). The time and position resolutions shown in this work compare favorably with the best time resolutions shown for TOF/DOI PET detectors in literature (see Table 1). However, unlike past high performance TOF/DOI PET modules, the modules presented in this work require only a single timing channel per module, and do not require active cooling or the acquisition of pulse shape information.

One issue requiring further investigation is the unusual geometry of the scintillation crystals used in this work. While crystal elements have traditionally been rectangular prisms, in this work the top layer of crystals used was made up of triangular prisms (see Figure 2). The effects of this geometry change on reconstructed images should be investigated in further works.

We note that if triangular prism scintillation crystals are not desired, the basic signal multiplexing principles presented in this work could be applied to many types of TOF/DOI crystal configurations. Other light sharing crystal array designs could theoretically be used with the binary position sensitive network so long as the light distribution on the SiPM array is unique for each scintillation crystal. Other crystal designs could lead to different position sensitivity or additional DOI layers. For each crystal array a binary network must be designed to avoid crystal overlap, and maximize the distance between crystals in the flood map.

5. Conclusions

A multiplexed TOF/DOI PET detector has been described and tested operating at room temerpature. Two layer DOI (10mm resolution) has been demonstrated using a passive binary positioning network and a two layer light sharing LYSO array. With a 20mm effective LYSO thickness 180 ± 2ps FWHM coincidence time resolution was achieved with four 3mm

× 3mm SiPMs multiplexed to a single timing channel. 204 ± 1ps FWHM coincidence time resolution was achieved with sixteen 3mm × 3mm SiPMs multiplexed. Excellent timing resolution was also demonstrated with a simple comparator readout. The detector architecture demonstrated in this paper is a promising method to greatly simplify TOF/DOI PET detectors while maintaining excellent performance.

Acknowledgments

This work was supported in part by NIH research grants R01EB011552, R25CA118681 and R21EB014405, and NIH training grant F31CA171573.

References

Bieniosek M, Cates J, Grant A, Levin C. Analog filtering methods improve leading edge timing performance of multiplexed sipms. Physics in Medicine and Biology. 2016; 61(16):N427. [PubMed: 27484131]

Bieniosek M, Cates J, Levin C. Achieving fast timing performance with multiplexed sipms. Physics in medicine and biology. 2016; 61(7):2879. [PubMed: 26987898]

Bieniosek, MF.; Cates, JW.; Levin, CS. Nuclear Science Symposium Conference Record (NSS/MIC), 20015 IEEE. IEEE; 2015. A light sharing, charge multiplexed time-of-flight depth-of-interaction pet detector; p. M4D1-M4D4.

Budinger TF. Time-of-flight positron emission tomography: status relative to conventional pet. Journal of nuclear medicine. 1983; 24(1):73–78. [PubMed: 6336778]

Downie E, Yang X, Peng H. Investigation of analog charge multiplexing schemes for sipm based pet block detectors. Physics in medicine and biology. 2013; 58(11):3943. [PubMed: 23680653]

Gariod R, Allemand R, Cormoreche E, Laval M, Moszynski M. The leti positron tomograph architecture and time of flight improvements. Proceedings of The Workshop on Time of Flight Tomography. 1982:25–29.

H-J, C. Nuclear Science Symposium Conference Record (NSS/MIC), 20014 IEEE. IEEE; 2014. Development of a tof detector for brain pet; p. M19-M25.

Ito M, Lee MS, Lee JS. Continuous depth-of-interaction measurement in a single-layer pixelated crystal array using a single-ended readout. Physics in medicine and biology. 2013; 58(5):1269. [PubMed: 23384966]

Kang HG, Ko GB, Rhee JT, Kim KM, Lee JS, Hong SJ. A dual-ended readout detector using a meantime method for sipm tof-doi pet. Nuclear Science, IEEE Transactions on. 2015; 62(5):1935–1943.

Karp JS, Surti S, Daube-Witherspoon ME, Muehllehner G. Benefit of time-of-flight in pet: experimental and clinical results. Journal of Nuclear Medicine. 2008; 49(3):462–470. [PubMed: 18287269]

Kim, C.; McDaniel, D.; Malaney, J.; McBroom, G.; Peterson, W.; Tran, VH.; Guo, J.; Ivan, A.; Dolinsky, S.; Wagadarikar, A., et al. Nuclear Science Symposium and Medical Imaging Conference (NSS/MIC), 2012 IEEE. IEEE; 2012. Time-of-flight pet-mr detector development with silicon photomultiplier; p. 3533-3536.

Kim H, Chen C-T, Eclov N, Ronzhin A, Murat P, Ramberg E, Los S, Wyrwicz A, Li L, Kao C-M. A feasibility study of a pet/mri insert detector using strip-line and waveform sampling data acquisition. Nuclear Instruments and Methods in Physics Research Section A. Accelerators, Spectrometers, Detectors and Associated Equipment. 2015; 784:557–564.

Kwon SI, Lee JS. Signal encoding method for a time-of-flight pet detector using a silicon photomultiplier array. Nuclear Instruments and Methods in Physics Research Section A. Accelerators, Spectrometers, Detectors and Associated Equipment. 2014; 761:39–45.

Levin CS. New imaging technologies to enhance the molecular sensitivity of positron emission tomography. Proceedings of the IEEE. 2008; 96(3):439–467.

Moses WW. Recent advances and future advances in time-of-flight pet. Nuclear Instruments and Methods in Physics Research Section A. Accelerators, Spectrometers, Detectors and Associated Equipment. 2007; 580(2):919–924.

Mullani NA, Markham J, Ter-Pogossian MM. Feasibility of time-of-flight reconstruction in positron emission tomography. J Nucl Med. 1980; 21(11):1095–1097. [PubMed: 6968822]

Roncali E, Schmall JP, Viswanath V, Berg E, Cherry SR. Predicting the timing properties of phosphor-coated scintillators using monte carlo light transport simulation. Physics in medicine and biology. 2014; 59(8):2023. [PubMed: 24694727]

Schmall JP, Surti S, Karp JS. Characterization of stacked-crystal pet detector designs for measurement of both tof and doi. Physics in medicine and biology. 2015; 60(9):3549. [PubMed: 25860172]

Spanoudaki VC, Levin C. Investigating the temporal resolution limits of scintillation detection from pixellated elements: comparison between experiment and simulation. Physics in medicine and biology. 2011; 56(3):735. [PubMed: 21239845]

Van Dam HT, Borghi G, Seifert S, Schaart DR. Sub-200 ps crt in monolithic scintillator pet detectors using digital sipm arrays and maximum likelihood interaction time estimation. Physics in medicine and biology. 2013; 58(10):3243. [PubMed: 23611889]

Vinke R, Yeom JY, Levin CS. Electrical delay line multiplexing for pulsed mode radiation detectors. Physics in medicine and biology. 2015; 60(7):2785. [PubMed: 25768002]

Yeom JY, Vinke R, Levin CS. Side readout of long scintillation crystal elements with digital sipm for tof-doi pet. Medical physics. 2014; 41(12):122501. [PubMed: 25471979]

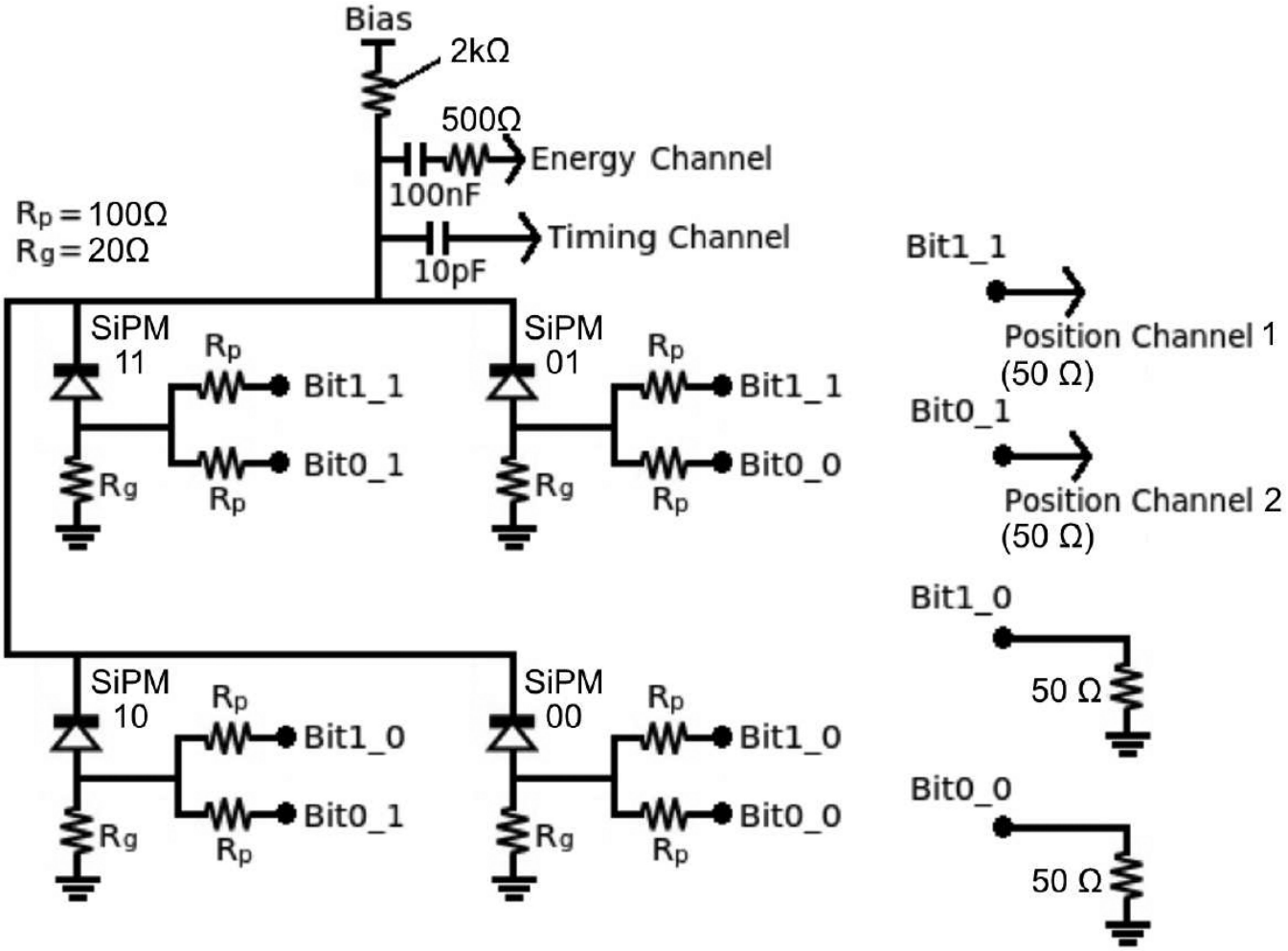

Figure 1.

Schematic of a 2 bit binary position sensitive network. Each SiPM cathode is multiplexed to a common timing and energy channel. Each anode is connected to a low impedance resistor to ground and 2 split off channels that are connected to position channels or dummy resistors in unique combinations.

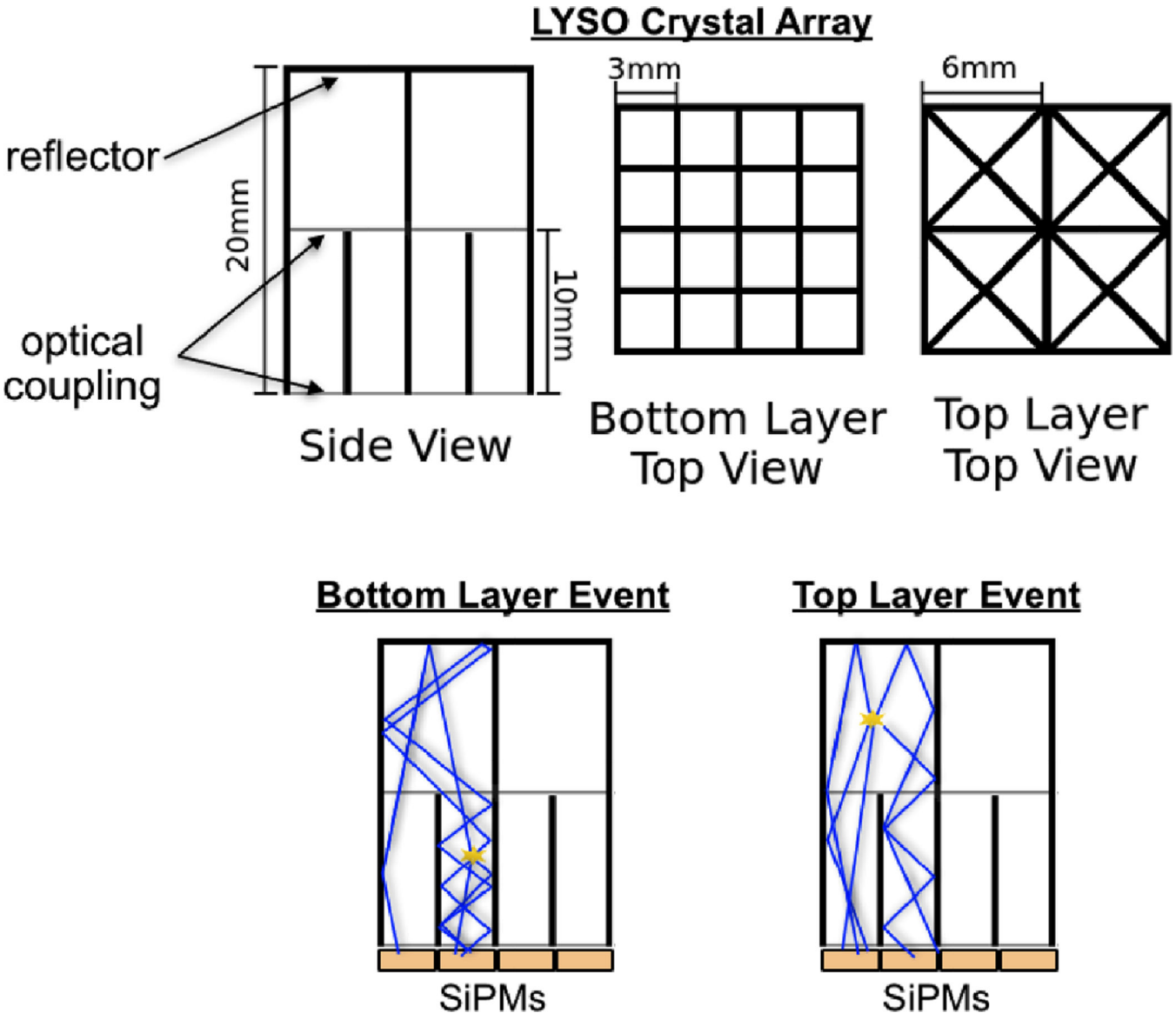

Figure 2.

The LYSO scintillation crystal array used in this work. Bottom layer scintillation event light is primarily detected by a single SiPM, while top layer scintillation light is primarily shared evenly between two SiPMs.

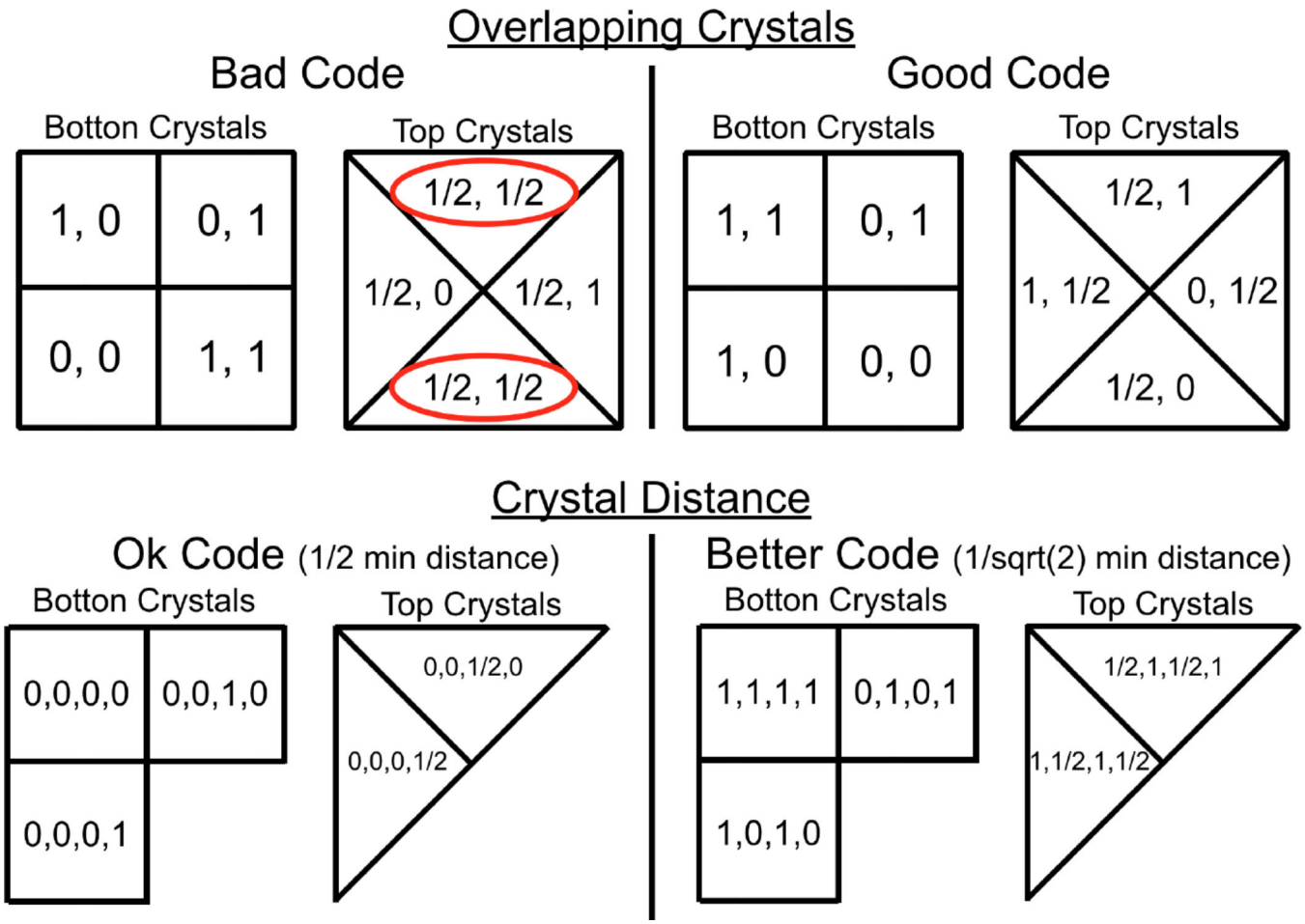

Figure 3.

Issues when designing binary codes with the light sharing crystal arrays described in paper. Since top layer crystals share light with two SiPMs, some binary code arrangements can have top layer crystals with overlapping codes (corresponding to overlap in the flood map), or codes with non-optimal crystal distance (leading to higher probability of crystal misidentification).

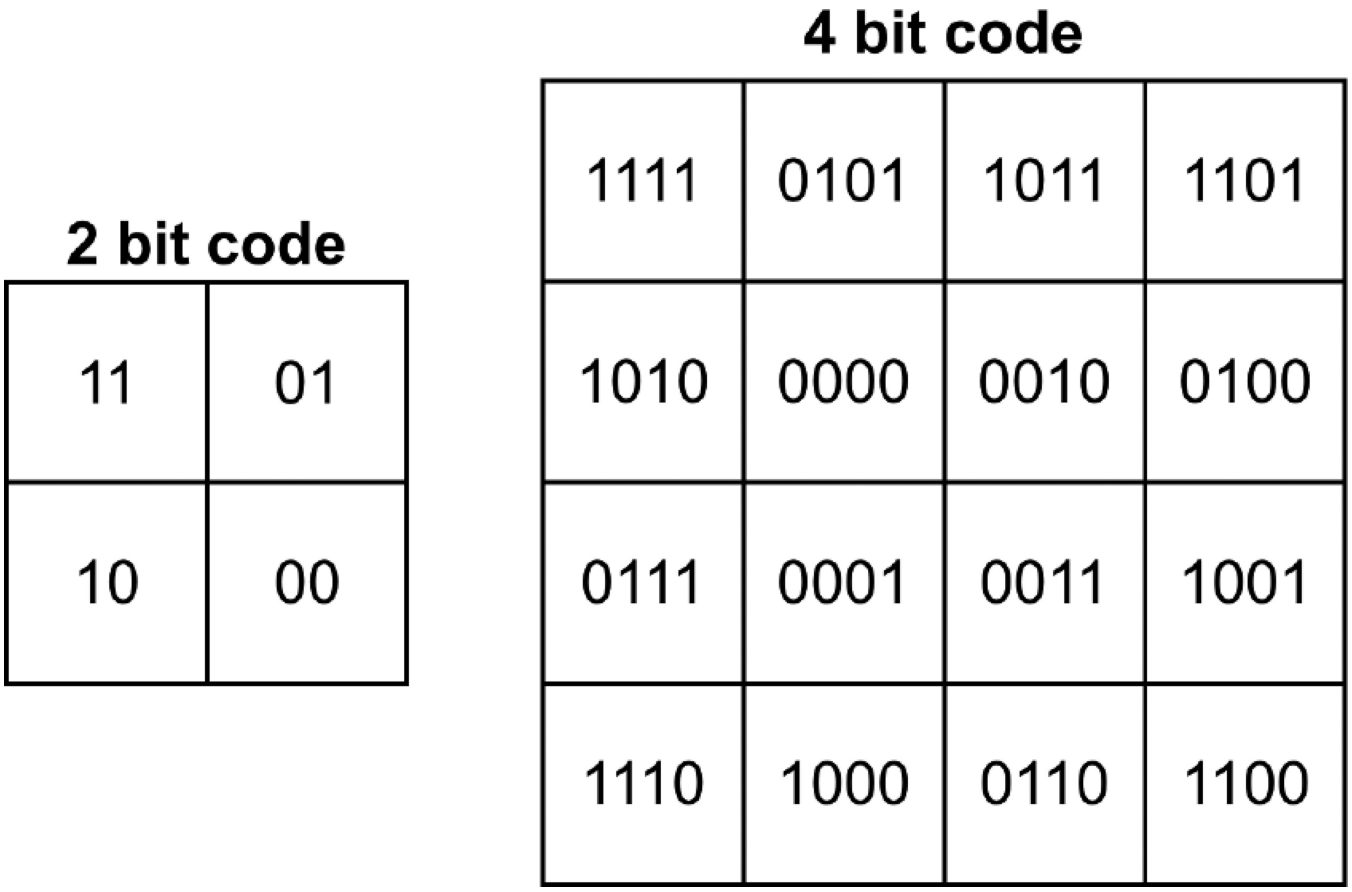

Figure 4.

Binary codes used for the 2 SiPMs in the 2 bit configuration (left) and 16 SiPMs in the 4 bit configuration (right) in this work. Each bit of the code corresponds to the connection of that SiPM's split off channel to a position channel (1) or a dummy resistor (0). The schematic representation of the 2 bit code is also seen in Figure 1.

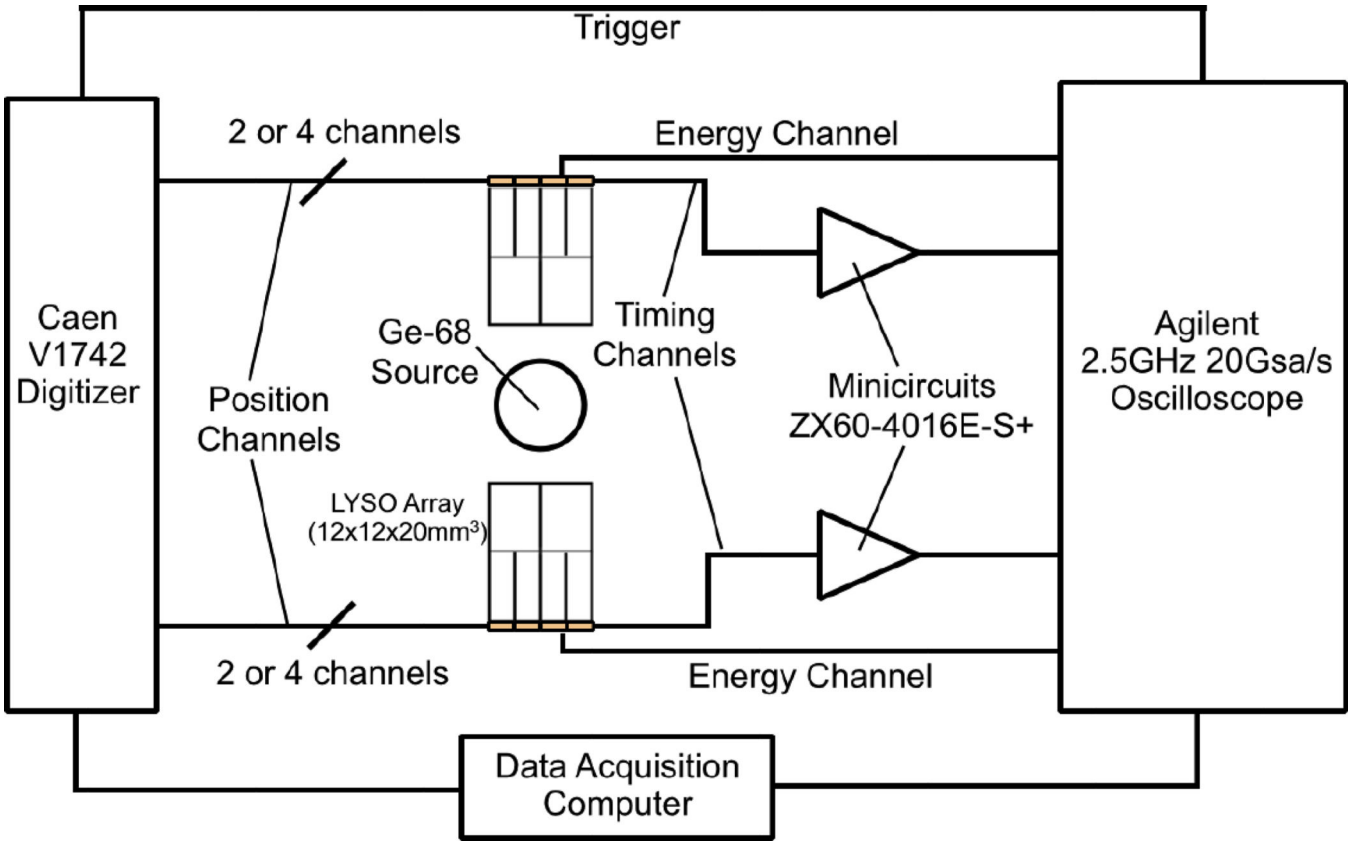

Figure 5.
Block diagram of the setup for DOI crystal array to DOI crystal array coincidence timing experiments with a sampling oscilloscope used for leading edge time pickoff.

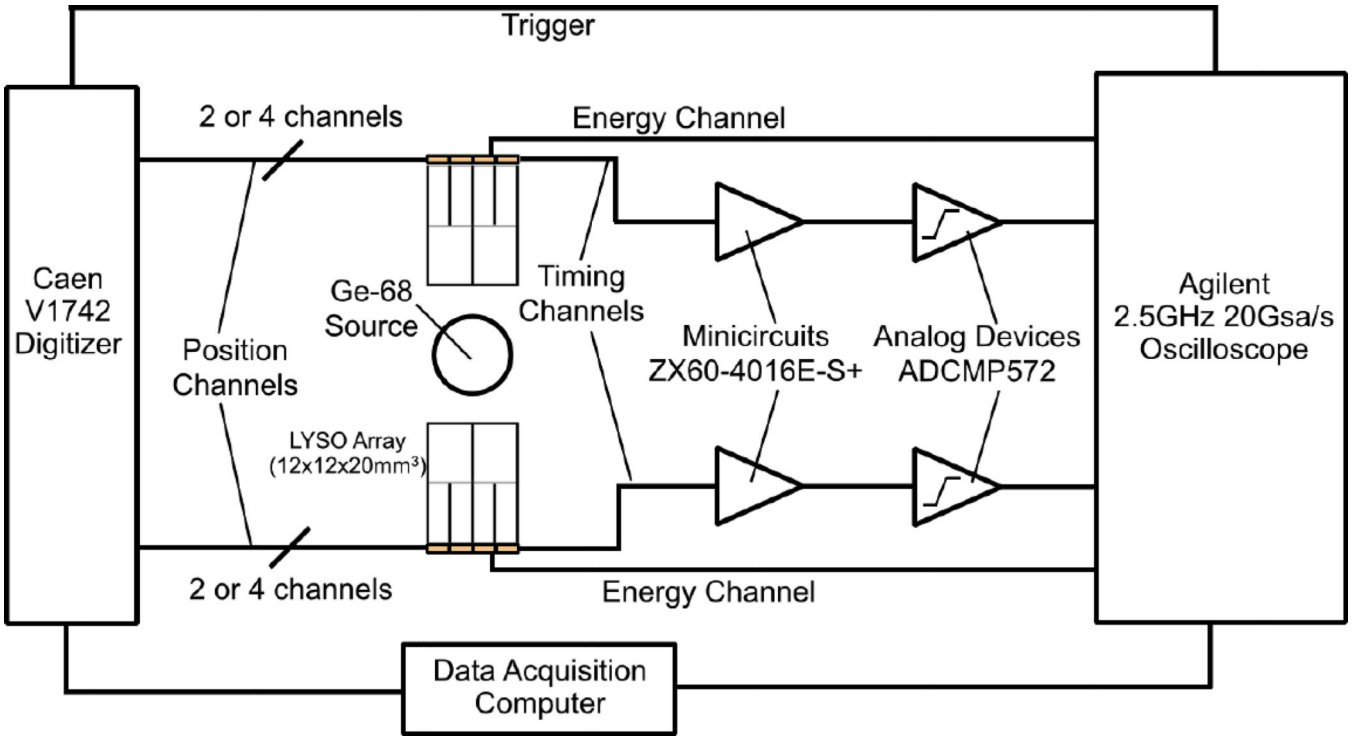

Figure 6.

Block diagram of the setup for coincidence timing experiments with an Analog Devices ADCMP572 comparator used for leading edge time pickoff that is scalable to a full PET system.

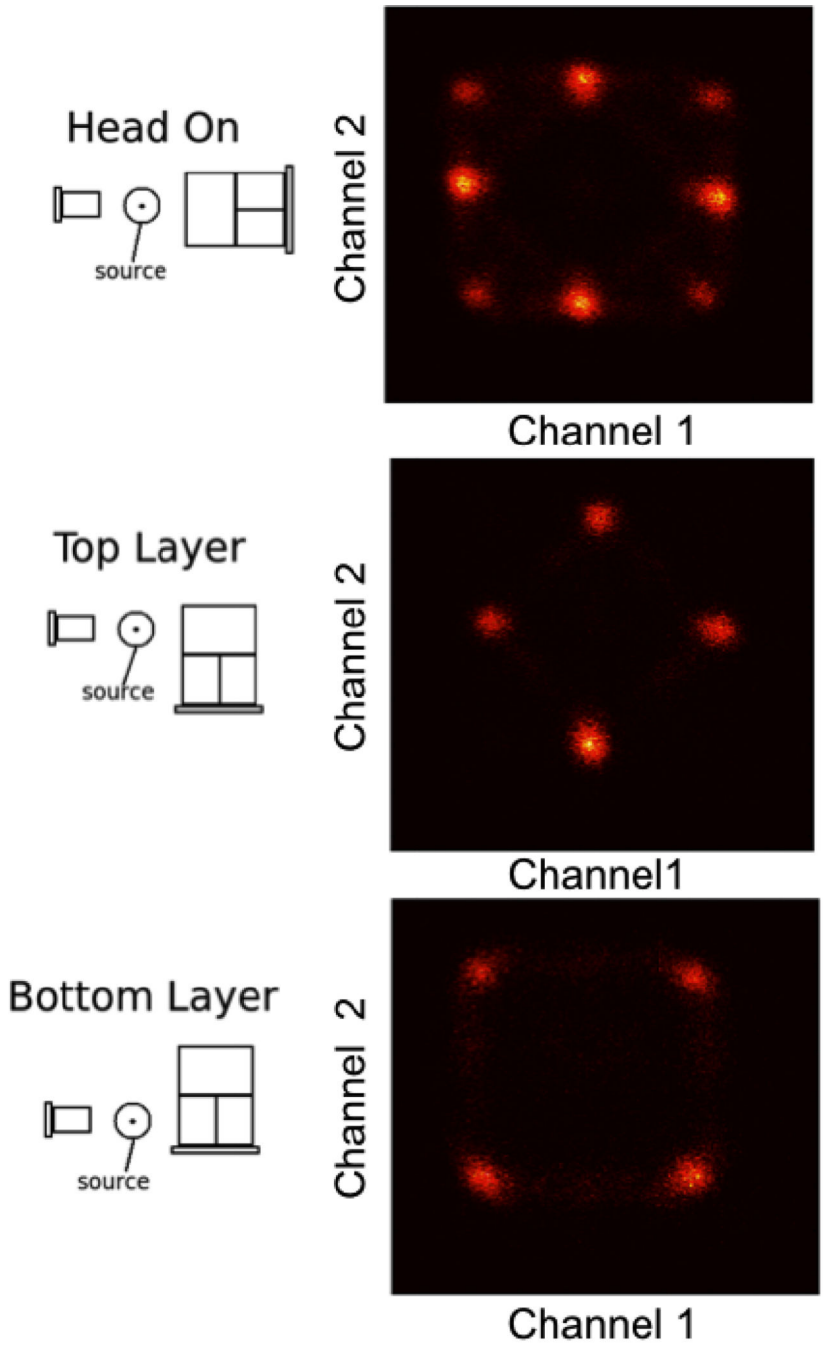

Figure 7.
Flood maps with a 2 bit binary network with head on, top layer and bottom layer collimation.

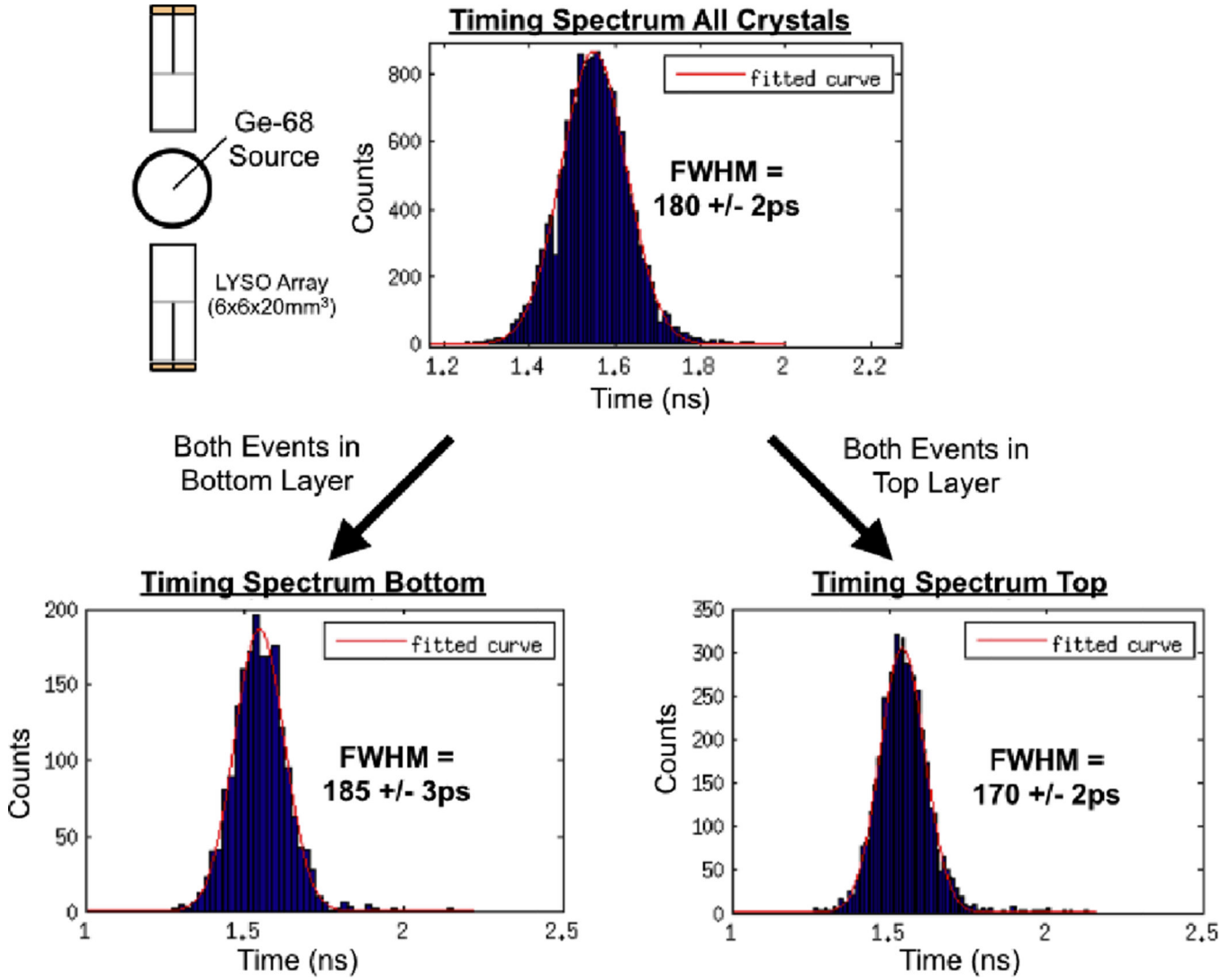

Figure 8.

Coincidence timing histograms for two detector modules each comprising 2×2=4 SiPMs multiplexed to a single timing channel and a 4 bit binary network setup. Timing histograms are shown for the all coincidence events (top), for events where both 511keV events were detected in bottom layer crystals (bottom left), and for events where both 511keV events were detected in top layer crystals (bottom right).

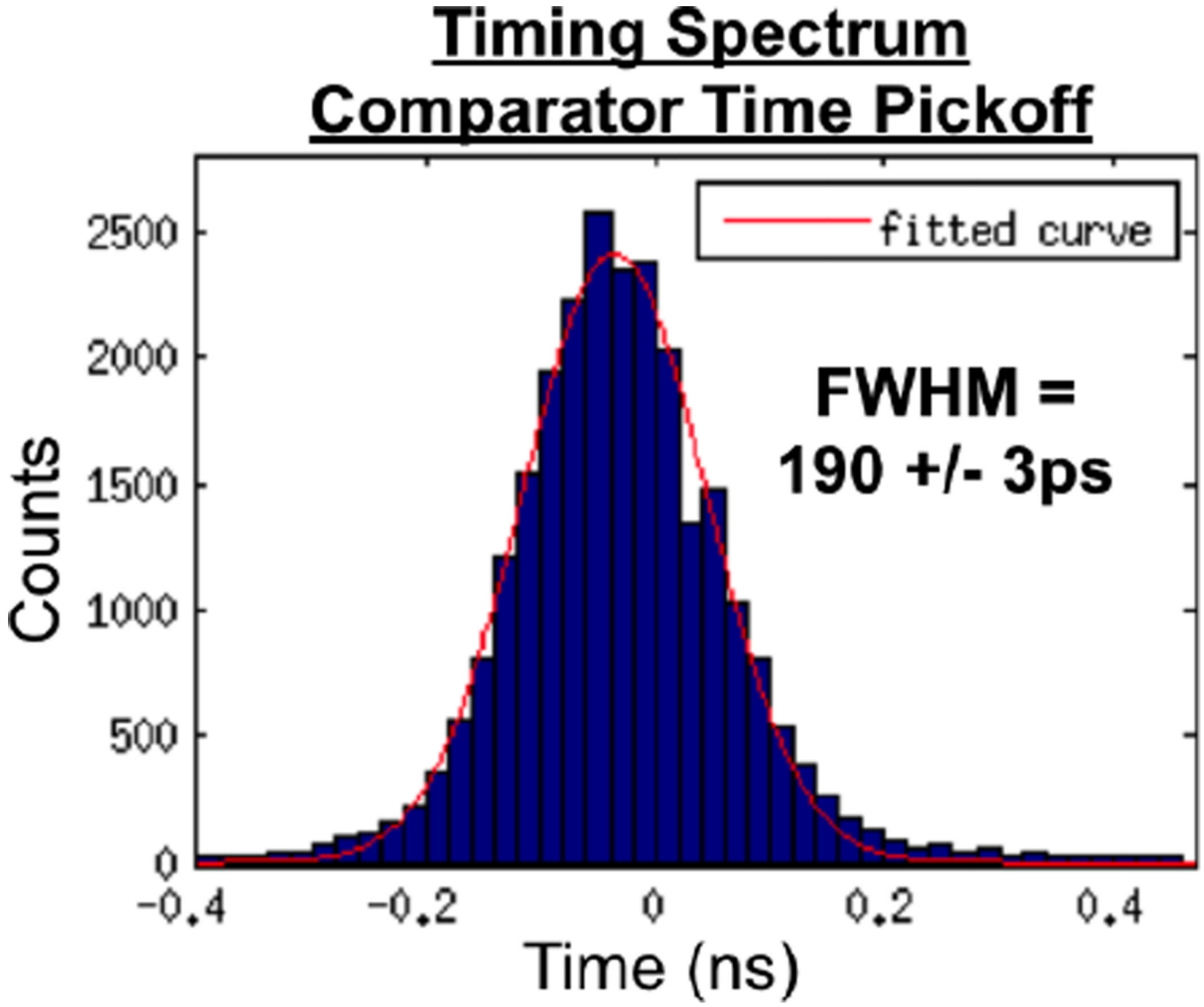

Figure 9.

Coincidence timing histogram with for two detector modules each of comprising of 2×2= 4 SiPMs multiplexed to a single timing channel with comparator time pickoff and a 2 bit binary network setup.

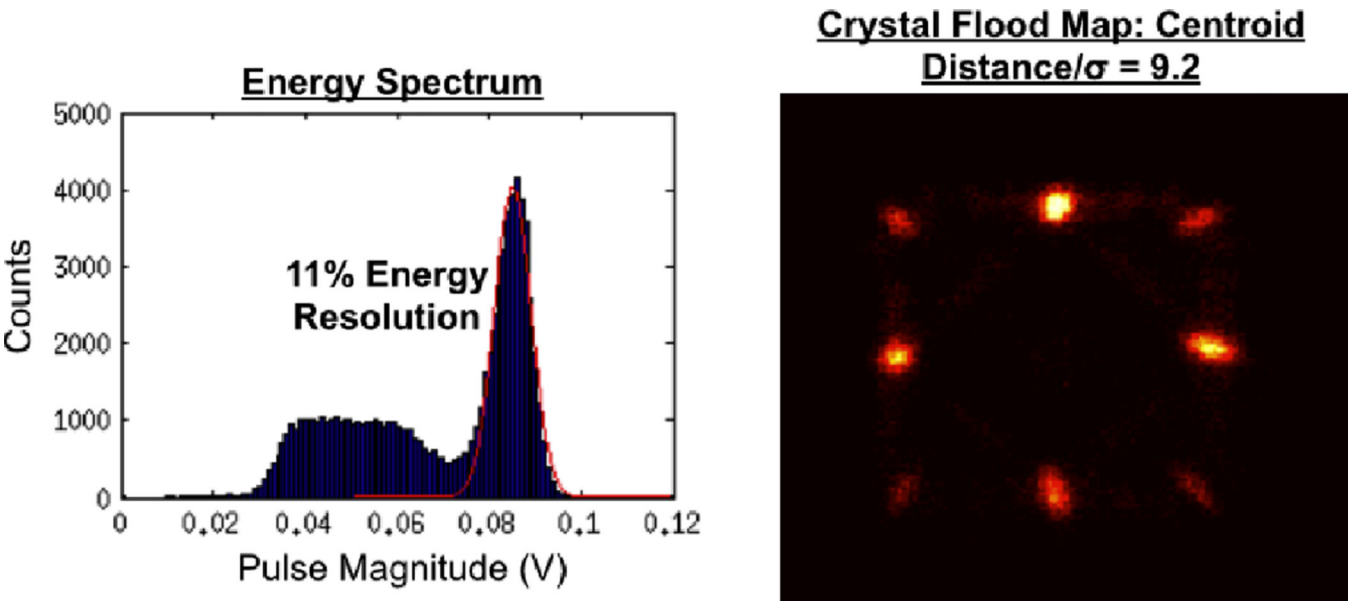

Figure 10.

Energy spectrum (all crystals) and flood histogram for a detector array based on a 2×2=4 SiPM array with a 2 bit binary positioning network. The axes of the flood map are the magnitudes of the position channels.

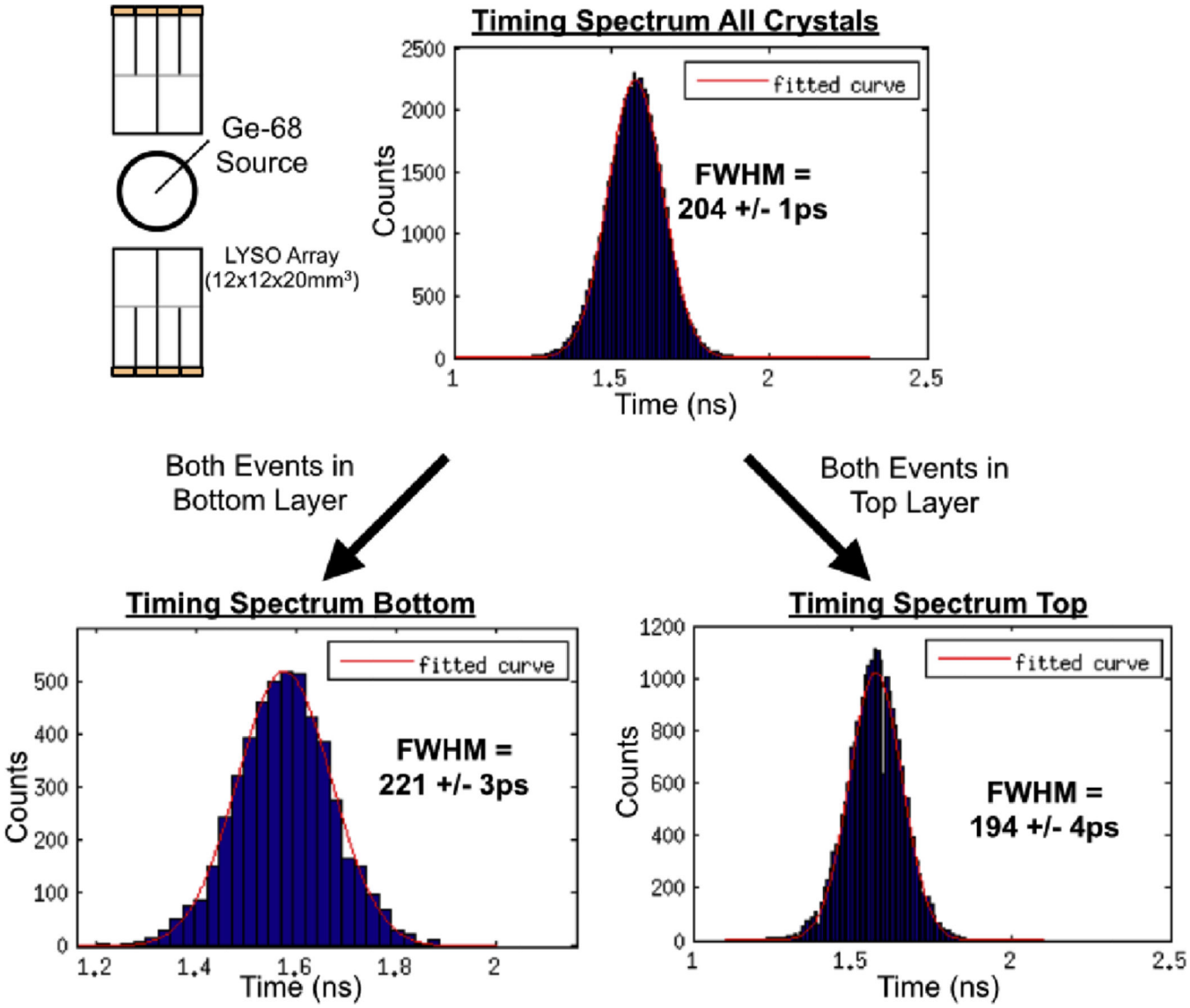

Figure 11.

Coincidence timing histograms for two detector modules each comprising of 4×4=16 SiPMs multiplexed to a single timing channel and a 4 bit binary network setup. Timing histograms are shown for the all coincidence events (top), for events where both 511keV events were detected in bottom layer crystals (bottom left), and for events where both 511keV events were detected in top layer crystals (bottom right).

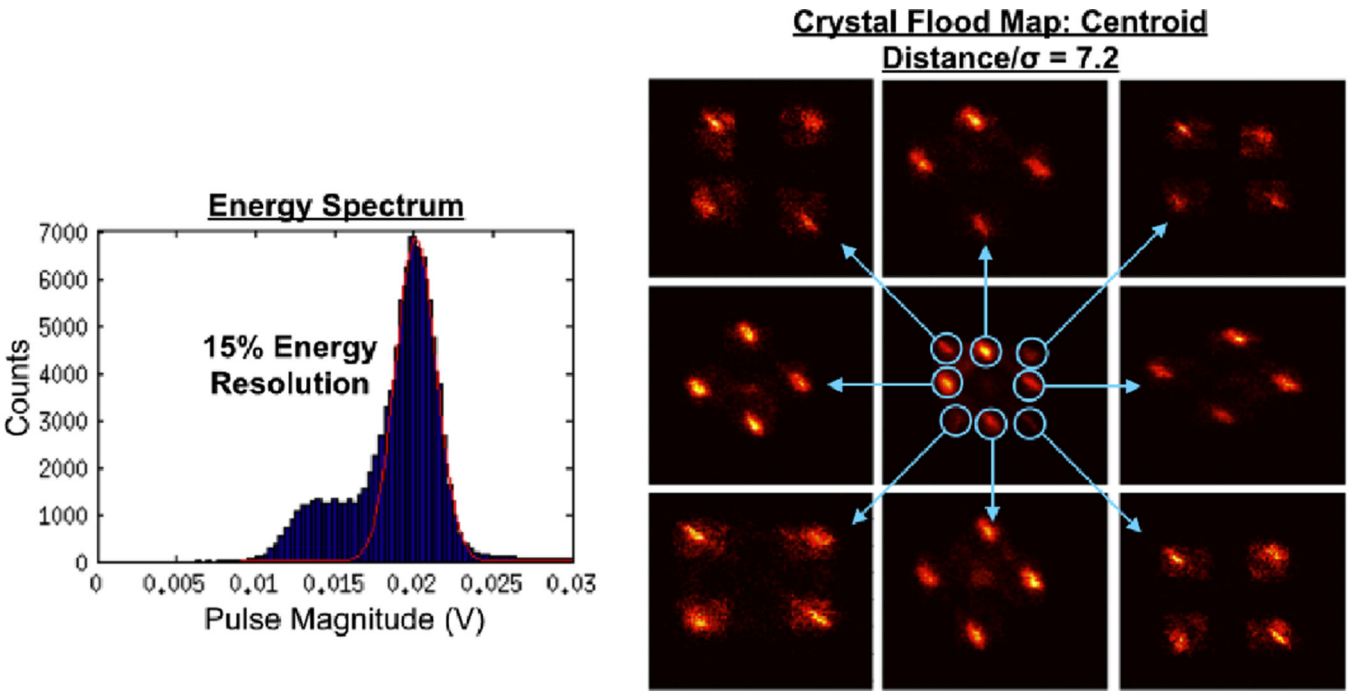

Figure 12.

Energy spectrum (all crystals) and flood histogram for a detector module based on a 4×4=16 SiPM array with a 4 bit binary positioning network. Since there are 4 position channels the flood map has 4 dimensions. To display the flood map, position channel 1 and 2 signal magnitudes are plotted in the center flood map. Each of the eight clusters in the center flood map show events from 4 crystals. These are seen when the channel 3 and 4 flood map of each cluster is plotted. These 8 outer flood maps show all 32 crystals in the array.

Table 1

Comparison of state of the art ToF-DOI approaches to this work.

	ToF DOI Approach			
	Monolithic (Van Dam et al. 2013)	**Phoswich (single crystal) (Schmall et al. 2015)**	**2 Bit Binary This Work**	**4 Bit Binary This Work**
Crystal	LYSO	CeBr3	LYSO	LYSO
Crystal Thickness	20mm	24mm	20mm	20mm
Time Resolution	184ps	153ps (average of layers)	180ps	204ps
DOI Resolution	1 to 4.5mm	12mm	10mm	10mm
Comments	−25 °C operation	Needs Pulse Shape Info	4:1 Multiplexed	16:1 Multiplexed